

# Inner core–mantle gravitational locking and the super-rotation of the inner core

Mathieu Dumberry<sup>1</sup> and Jon Mound<sup>2</sup>

<sup>1</sup>*Department of Physics, University of Alberta, Edmonton, Canada. E-mail: dumberry@ualberta.ca*

<sup>2</sup>*School of Earth & Environment, University of Leeds, Leeds, UK*

Accepted 2010 February 11. Received 2010 February 11; in original form 2009 August 14

## SUMMARY

Seismological observations suggest that the Earth's solid inner core has been rotating faster than the mantle over the past several decades, consistent with the results of some numerical geodynamo models. However, the hemispherical anisotropy structure of the inner core, also seismically observed, may require the inner core to remain at a relatively fixed longitudinal alignment with respect to the mantle, perhaps due to gravitational locking between them. Both of these seismic observations may be compatible if the differential rotation of the inner core is oscillatory in nature, with no mean offset over geologically long timescales. In this work, we investigate the possible rates of rotation of an oscillating inner core and the dynamics of coupling within the core–mantle system from an angular momentum perspective. We find that gravitational coupling between the inner core and mantle acts to prevent differential rotation, although the period at which 'locking' occurs differs depending on which of the inner core or mantle is driving the motion. We also show that for an internally generated torque, a long period (longer than 100 yr) oscillation of the inner core with a rate equal to  $0.25^\circ \text{ yr}^{-1}$ , on the high end of the rates inferred from seismic observations, is possible. However, the mantle oscillations entrained by gravitational coupling in such a scenario are only marginally compatible with the observed changes in length of day. We show that, in order to explain the seismically inferred rotation rates, either the gravitational coupling must be lower than previous estimates, or the electromagnetic coupling at the core–mantle boundary must be stronger than typical estimates.

**Key words:** Earth rotation variations; Dynamo: theories and simulations; Core, outer core and inner core.

## 1 INTRODUCTION

Numerical models of the geodynamo have found that motion of the fluid core near the inner core boundary (ICB) can produce electromagnetic (EM) torques on the inner core such that the latter would rotate faster than the mantle (Glatzmaier & Roberts 1996). Seismic evidence in support of an eastward inner core super-rotation has been found subsequently using different techniques (see the reviews by Tromp 2001; Song 2003). The most recent estimate comes from repeated event/receiver configurations (earthquake doublets) for which temporal variations in seismic waveform are interpreted to reflect differential inner core rotation (Zhang *et al.* 2005). Rates of inner core rotation inferred from this technique are of the order of  $0.2\text{--}0.5^\circ \text{ yr}^{-1}$ , on the high end of the range of various seismic estimates.

A differentially rotating inner core at a rate of  $0.2\text{--}0.5^\circ \text{ yr}^{-1}$  is difficult to reconcile with the presence of non-spherical density structures in the mantle and inner core; gravitational interaction between these should act to prevent relative rotation between the

two (Buffett 1996). A steady inner core rotation could exist, but only provided the inner core can deform viscously (Buffett 1997). For steady rates to be as high as  $0.2^\circ \text{ yr}^{-1}$ , viscous deformations must occur on a relatively rapid timescale of  $\sim 5\text{--}10 \text{ yr}$  (Dumberry 2007).

However, a persistent super-rotation of the inner core over geologically long timescales remains difficult to reconcile with another seismic observation, the observed longitudinal (hemispherical) anisotropy structure of the inner core (Tanaka & Hamaguchi 1997; Niu & Wen 2001). The origin of such structure is unknown, though it is likely connected to longitudinal variations in outer core dynamics, either causing lateral variations in plastic deformation or texturing the inner core during solidification (Sumita & Bergman 2007). In turn, relatively stationary patterns in core convection are likely connected to heat flux variations at the core–mantle boundary (CMB) (Willis *et al.* 2007; Sreenivasan & Gubbins 2008) and indeed may produce lateral variations in heat flux at the ICB resulting in uneven growth of the inner core (Aubert *et al.* 2008). Although at present we do not know the mechanism responsible for

the inner core hemispherical anisotropy, if it results from such a dynamic connection to the mantle or the CMB, it requires the inner core to remain in a relatively fixed orientation with respect to the mantle.

A possible scenario that allows the inner core to be currently in super-rotation while remaining in alignment with the mantle over geological timescales is if its rotation is not steady but instead represents a long period oscillation. Since seismic observations suggest an eastward rotation for the past 30 yr, the period or typical timescale of an oscillating inner core would have to be at least several decades. Possible rates of rotation of an oscillating inner core were considered by Dumberry (2007) from a geodynamic perspective, based on a simple dynamic model of angular momentum exchanges between the mantle, fluid core and inner core. This study showed that the rotation rate of an oscillating inner core is constrained by the fluctuations in mantle rotation induced by gravitational coupling, which must not exceed observed length of day (LOD) variations. Subject to this constraint, oscillating inner core rates as high as  $0.2^\circ \text{ yr}^{-1}$  could be achieved, though only provided the strength of the gravitational coupling is lower than previous estimates [based on the study of Mound & Buffett (2006)] or if the strength of EM coupling at the CMB is higher than that expected from typical values of lower mantle conductance and magnetic field strength.

However, an important limitation of the the model of Dumberry (2007) is that the fluid core region was over simplified. It was simply divided in two regions (separated by the tangent cylinder) and no differential fluid motion was allowed within each of these regions (i.e. they were considered as rigid bodies). A more realistic description of the fluid core could affect the angular momentum dynamics and the possible rates of inner core oscillation. Indeed, decadal timescale axially invariant, axisymmetric, zonal core flows in the form of cocentric cylinders can be inferred by combining magnetic field and LOD observations (Jault *et al.* 1988; Jackson *et al.* 1993). This type of fluid motion is predicted by theory (Taylor 1963) and may correspond to normal modes of oscillations between cylinders referred to as torsional oscillations (Braginsky 1970; Zatman & Bloxham 1997). Because of strong EM coupling at the ICB, these ‘rigid zonal flows’ should efficiently entrain the inner core in their motion and may thus possibly affect its rate of oscillation. An internal angular momentum model that allows for such flows may then alter the conclusions reached by Dumberry (2007), in particular at periods that are close to those of the torsional oscillations normal modes where resonance can occur.

In this study, we revisit the possible rates of rotation of an oscillating inner core. We expand upon the work of Dumberry (2007) by allowing differential rotation of cylinders within the fluid core. We then investigate the possible rates of inner core super-rotation that can be achieved in this more complete dynamic scenario.

Our model permits a more general investigation of the differential rotation that can exist within the core–mantle system. If coupling between two regions is sufficiently strong, differential motion is small and the two regions are ‘locked’ together, that is they undergo corotation. For a given set of coupling parameters, whether two regions are locked depends on the frequency of the forcing. But, as we illustrate below, it depends also on which region is responsible for driving the oscillations. Thus, following the description of our model in the next section, in Section 3 we investigate ‘locking’ between different regions of the core–mantle system. Such locking scenarios are instructive to elucidate the fundamental dynamics of the system and to understand the limits on the rate of inner core differential rotation with respect to the mantle. The latter issue, being the main motivation for this study, is investigated in Section 4.

## 2 ANGULAR MOMENTUM MODEL

We consider the problem from an angular momentum perspective. In the absence of external torques the equations governing the axial angular momentum of the mantle, inner core and fluid core are given, respectively, by

$$\frac{d}{dt} C_m \Omega_m = \Gamma_{\text{cmb}} - \Gamma_g, \quad (1)$$

$$\frac{d}{dt} C_i \Omega_i = \Gamma_{\text{icb}} + \Gamma_g, \quad (2)$$

$$\frac{d}{dt} \int_V c_f \omega_f dV = -\Gamma_{\text{cmb}} - \Gamma_{\text{icb}}, \quad (3)$$

where  $C_m$  and  $\Omega_m$  are, respectively, the axial moment of inertia and rotation rate of the mantle and  $C_i$  and  $\Omega_i$  are those for the inner core.  $c_f$  is the axial moment of inertia density within the volume  $V$  of the fluid core and  $\omega_f$  is the angular velocity of fluid parcels. The entire system is assumed to rotate at a steady background rate of  $2\pi$  per day and the angular velocities are taken to be departures from this state. We consider only axial torques and rotations in this study, that is torques that act to alter the magnitude but not the orientation of the rotation vectors.  $\Gamma_{\text{cmb}}$  and  $\Gamma_{\text{icb}}$  are the torques from all surface forces acting on the mantle at the CMB and on the inner core at the ICB, respectively.

$\Gamma_g$  is the gravitational torque exerted by the mantle on the inner core and depends on the rotational misalignment of the inner core and mantle density fields. For a small angle of misalignment  $\alpha$ , the gravitational torque of the mantle on the inner core is given by

$$\Gamma_g = -\bar{\Gamma}\alpha, \quad (4)$$

where  $\bar{\Gamma}$  is a proportionality constant that may be obtained from a mantle density model (Buffett 1996). The time variation of the misalignment angle  $\alpha$  is related to the differential rotation between the inner core and the mantle. Additionally, it is also related to the rate at which viscous relaxation of the inner core allows its density structure to adjust to the misaligned gravitational potential imposed by the mantle. We assume that the inner core deforms as a simple Newtonian viscous fluid, in which case its rate of relaxation is proportional to the misalignment angle. The time-evolution of  $\alpha$  is thus determined by

$$\frac{d\alpha}{dt} = \Omega_i - \Omega_m - \frac{\alpha}{\tau}, \quad (5)$$

where  $\tau$  is the characteristic timescale of viscous relaxation. Using the mapping provided by Buffett (1997),  $\tau = 1 \text{ yr}$  corresponds to a bulk inner core viscosity of  $\eta_s = 5 \times 10^{16} \text{ Pa s}$ .

Let us first consider the modes of oscillation that are possible in a simplified system of a gravitationally coupled mantle and inner core. For this initial exercise, we further assume a perfectly rigid inner core (i.e.  $\tau = \infty$ ) and we neglect coupling at the CMB and ICB (i.e.  $\Gamma_{\text{cmb}} = \Gamma_{\text{icb}} = 0$ ). With these approximations, the fluid core is decoupled from the inner core and mantle and has to conserve its own angular momentum. Taking time-derivatives of (1) and (2) and using (4) and (5), we can write the above system of equations as

$$\frac{d^2}{dt^2} C_m \Omega_m = \bar{\Gamma}(\Omega_i - \Omega_m), \quad (6)$$

$$\frac{d^2}{dt^2} C_i \Omega_i = -\bar{\Gamma}(\Omega_i - \Omega_m), \quad (7)$$

**Table 1.** Parameters used in calculations.

Parameter	Symbol	Value
Radius of ICB	$r_i$	$1.22 \times 10^6$ m
Radius of CMB	$r_f$	$3.48 \times 10^6$ m
Core conductivity	$\sigma$	$5 \times 10^5$ S m <sup>-1</sup>
Gravitational torque coefficient	$\bar{\Gamma}$	$3 \times 10^{20}$ N m
Inner core viscous relaxation time	$\tau$	1–1000 yr
Conductance at base of mantle	$G_m$	$10^8$ S
Axial moment of inertia of		
Mantle	$C_m$	$7.12 \times 10^{37}$ kg m <sup>2</sup>
Inner core	$C_i$	$5.87 \times 10^{34}$ kg m <sup>2</sup>
Fluid within tangent cylinder	$C_c$	$2.27 \times 10^{35}$ kg m <sup>2</sup>
Fluid outside tangent cylinder	$C_o$	$8.91 \times 10^{36}$ kg m <sup>2</sup>
Radial magnetic field		
Rms of axial dipole at CMB	$\langle B_m^d \rangle$	0.226 mT
Rms of radial field at CMB	$\langle B_m^r \rangle$	0.319 mT
Rms of axial dipole at ICB	$\langle B_i^d \rangle$	2.0 mT
Rms of radial field at ICB	$\langle B_i^r \rangle$	3.0 mT
Cylindrically in fluid	$B_s$	0.3 mT

which is an eigenvalue problem for coupled simple harmonic oscillators. Solutions of this system gives the natural frequencies and their associated eigenvectors  $[\Omega_m, \Omega_i]$

$$\omega_0 = 0 \quad [1, 1]$$

$$\omega_0 = \sqrt{\frac{\bar{\Gamma}(C_m + C_i)}{C_m C_i}} \quad \left[1, -\frac{C_m}{C_i}\right].$$

The first solution is the trivial case of non-oscillatory corotation and the second solution is the free oscillation that arises due to mantle-inner core gravitational (MICG) coupling. The period of the MICG mode depends on the strength of the gravitational coupling incorporated in the parameter  $\bar{\Gamma}$ . Taking  $3 \times 10^{20}$  N m (e.g. Buffett 1996; Mound & Buffett 2006) and using the moments of inertia (e.g. Stacey 1992) given in Table 1 gives a MICG period of 2.8 yr.

At periods greater than about 1 yr, strong EM coupling at the ICB locks the fluid within the tangent cylinder to the inner core (Gubbins 1981; Dumberry & Buffett 1999; Mound & Buffett 2003), such that all material within the tangent cylinder effectively rotates as a single rigid body. If this is the case, we should replace  $C_i$  in the above equations with  $C_i + C_c$ , where  $C_c$  is the axial moment of inertia of the fluid core within the tangent cylinder; the period of the MICG then lengthens to 6.1 yr (Mound & Buffett 2003). Indeed, a periodic 6-yr signal is observed in the LOD variations (Abarca del Rio *et al.* 2000) and has been interpreted to represent the MICG mode (Mound & Buffett 2006). If this interpretation is correct,  $\bar{\Gamma}$  cannot depart much from  $3 \times 10^{20}$  N m and we have chosen this value for most of our calculations in Sections 3 and 4. In addition, it also suggests that the viscous relaxation timescale of the inner core  $\tau$  cannot be much smaller than  $\sim 5$  yr, otherwise the MICG mode should be rapidly attenuated and not observed.

Since  $C_m \gg (C_i + C_c)$ , it is possible to approximate the MICG mode as one in which the inner core oscillates with respect to a stationary mantle with a frequency  $\omega \approx \sqrt{\bar{\Gamma}/(C_i + C_c)}$ . This approximate result could also be obtained if one were to assume from the outset that, due to the large difference in moments of inertia, the mantle should remain relatively stationary. That is, one could assume that  $\Omega_i \gg \Omega_m$  in eq. (7), leading to the approximate solution described above. Alternatively, one could suppose a situation in which the inner core was held stationary (by some torque not yet included in the model) and the mantle oscillated about this fixed inner core. In such a case one would set  $\Omega_i = 0$  in eq. (6) and obtain a frequency of oscillation  $\omega = \sqrt{\bar{\Gamma}/C_m}$ . Using the parameters

given in Table 1, this corresponds to a period of 97 yr. This is not a normal mode of the system described by eqs (6) and (7) as it requires the inner core to be held fixed by some external torque. However, this period marks the point at which the gravitational torque on the mantle from an oscillating inner core becomes larger than the rotational inertia of the mantle. It is thus connected to the ability of an oscillating inner core to entrain the mantle by gravitational coupling, as we investigate in more detail in Section 3.

We now return to the complete equations of axial angular momentum exchange (1)–(5) and consider the fluid core in more detail. We divide the fluid core into a large number of separate, co-axial cylinders (1000 for the models presented here). Each cylinder can rotate independently and must satisfy its own angular momentum balance. We give here a brief description of this balance; more details can be found for example in Buffett (1998) and Mound & Buffett (2003, 2005). When the angular velocity of a cylinder  $\Omega_f(s)$  at cylindrical radius  $s$  is proportional to  $\exp(-i\omega t)$ , where  $\omega$  is the frequency of oscillation, it must obey (Braginsky 1970)

$$-\omega^2 m(s) \Omega_f(s) = \frac{d}{ds} \left[ \mathcal{T}(s) \frac{d}{ds} \Omega_f(s) \right] + i\omega [f_i(s) + f_m(s)], \quad (8)$$

where

$$m(s) = 4\pi\rho s^3(z_f - z_i), \quad (9)$$

is the moment of inertia density of the cylinders, in which  $z_f = \sqrt{r_f^2 - s^2}$  and  $z_i = \sqrt{r_i^2 - s^2}$  where  $r_f$  and  $r_i$  are the spherical radius of the fluid core and inner core, respectively. We note that  $z_i = 0$  when  $s > r_i$ . The parameter  $\mathcal{T}(s)$  in (8) is a magnetic tension given by

$$\mathcal{T}(s) = \frac{4\pi}{\mu_o} s^3 (z_f - z_i) B_s^2, \quad (10)$$

where  $\mu_o$  is the magnetic permeability and  $B_s$  represents the (cylindrically) radial magnetic field averaged over the cylinder surface. When neighbouring cylinders undergo differential rotation, this magnetic tension acts as a restoring force trying to bring the cylinders back into alignment. We have chosen a value of  $B_s = 0.3$  mT; this choice leads to natural oscillations in  $\Omega_f(s)$  (the free modes of torsional oscillations) with longest periods of the order of a few decades. This is consistent with the interpretation that observed decadal rigid zonal core flows represent these free modes (e.g. Braginsky 1970; Zatman & Bloxham 1997; Buffett *et al.* 2009).

The parameters  $f_m(s)$  and  $f_i(s)$  in (8) capture the coupling of the cylinders to the CMB and ICB, respectively. They are related to  $\Gamma_{\text{cmb}}$  and  $\Gamma_{\text{icb}}$  that appear in (1)–(3) by

$$\Gamma_{\text{cmb}} = \int_0^{r_f} f_m(s) ds, \quad (11)$$

$$\Gamma_{\text{icb}} = \int_0^{r_i} f_i(s) ds. \quad (12)$$

Here we are interested in the part of this coupling that arises from axial differential motion of the fluid core with respect to the mantle and inner core. Consequently, we write (Buffett 1998)

$$f_m(s) = \mathcal{F}_m(s)[\Omega_f(s) - \Omega_m], \quad (13)$$

$$f_i(s) = \mathcal{F}_i(s)[\Omega_f(s) - \Omega_i]. \quad (14)$$

The form of the coupling parameters  $\mathcal{F}_m(s)$  and  $\mathcal{F}_i(s)$  depends on the nature of the torque. Coupling at the ICB is likely to be dominated by

EM forces (e.g. Gubbins 1981). A variety of coupling mechanisms have been suggested to be important at the CMB, though if there is a high-conductivity layer in the lower-most mantle (as inferred from nutation studies, e.g. Mathews *et al.* 2002), EM forces are also likely to dominate the coupling. Other coupling mechanisms can be incorporated in our framework, but for reasons of conciseness and tractability, here we restrict our attention to EM coupling at both the CMB and ICB.

EM coupling at a fluid–solid boundary depends on the morphology of the magnetic field as well as on the conductivity structure on the solid side of the boundary. The coupling parameters  $\mathcal{F}_m(s)$  and  $\mathcal{F}_i(s)$  incorporate this information. Explicit calculations of  $\mathcal{F}_m(s)$  for given magnetic field models at the CMB can be found in Dumberry & Mound (2008). The latter study also showed that a very good approximation of  $\mathcal{F}_m(s)$  is obtained when the magnetic field at the CMB is expressed simply in terms of its axial dipole part and the rms component of the radial field. We follow this prescription here and express the coupling at the CMB as (see Dumberry & Mound 2008)

$$\mathcal{F}_m(s) = 2\pi s^3 \left[ (B_m^d)^2 + \langle B_m^m \rangle^2 \right] G_m \left( \frac{r_f}{z_f} \right). \quad (15)$$

In this last equation,  $G_m$  is the conductance of the lower-most mantle, for which we assign a value of  $10^8$  S. This is compatible with the conductance required to explain a part of the observed nutations of the Earth (e.g. Mathews *et al.* 2002). We note that in the context of nutations,  $G_m = 10^8$  S represents an upper bound of the conductance that can be sampled on a diurnal timescale. The actual conductance may thus be larger than  $10^8$  S though we do not have supporting evidence for this. The quantity  $\langle B_m^m \rangle$  is the rms value of the total radial field at the CMB (including the axial dipole contribution) and  $B_m^d$  is the axial dipole radial field at the CMB. The latter is written in terms of the degree one, order zero gauss coefficient  $g_1^0$ , and given by (Gubbins & Roberts 1987)

$$B_m^d = 2 \left( \frac{r_a}{r_f} \right)^3 g_1^0 \cos \theta. \quad (16)$$

We note that this expression is a function of  $s$  through the colatitude angle  $\theta$ . We use values for both the axial dipole and total rms strength that are based on a time average of the *gufml* model of Jackson *et al.* (2000) over the period 1950–1990. Our adopted values are given in Table 1, where we also express the axial dipole amplitude in terms of its rms strength, that is

$$\langle B_m^d \rangle = \frac{2}{\sqrt{3}} \left( \frac{r_a}{r_f} \right)^3 g_1^0. \quad (17)$$

The combination of  $G_m = 10^8$  S and the values of  $\langle B_m^m \rangle$  and  $\langle B_m^d \rangle$  listed in Table 1 produce what we refer to here as a ‘typical’ EM coupling strength at the CMB.

Similarly, the EM coupling at the ICB can be expressed as (see Dumberry & Mound 2008)

$$\mathcal{F}_i(s) = 2\pi s^3 \left[ (B_i^d)^2 + \langle B_i^m \rangle^2 \right] G_i \left( \frac{r_i}{z_i} \right), \quad (18)$$

where  $B_i^d$  and  $\langle B_i^m \rangle$  refer to the axial dipole and rms components of the radial magnetic field at the ICB.  $B_i^d$  is related to its rms strength  $\langle B_i^d \rangle$  by a relation equivalent to that of (16) and (17). The conductance factor  $G_i$  incorporates the details of the magnetic field perturbation created by the shear at the ICB (e.g. Buffett 1998) and is given by

$$G_i = \frac{1}{4} [1 + i \operatorname{sgn}(\omega)] \sigma_f \delta_f, \quad (19)$$

where  $\sigma_f$  is the conductivity of the fluid core (assumed equal to that of the inner core,  $5 \times 10^5$  S m<sup>-1</sup> e.g. Stacey & Anderson 2001),  $\delta_f = \sqrt{2/\omega\mu_0\sigma_f}$  is the skin depth in the fluid core,  $\omega$  is the frequency of oscillation and  $\operatorname{sgn}(\omega) = \omega/|\omega|$ . It is useful to write the ICB EM coupling in the form

$$\mathcal{F}_i(s) = \frac{[1 + i \operatorname{sgn}(\omega)]}{\sqrt{\omega}} \hat{\mathcal{F}}_i(s), \quad (20)$$

where

$$\hat{\mathcal{F}}_i(s) = \sqrt{\frac{\sigma_f}{2\mu}} \pi s^3 \left[ (B_i^d)^2 + \langle B_i^m \rangle^2 \right] \left( \frac{r_i}{z_i} \right). \quad (21)$$

Due to a lack of direct, observational constraints for the geometry of the magnetic field at the ICB we have adopted field components (Table 1) having a similar geometry to the CMB magnetic field components, but with a total intensity that is greater by approximately an order of magnitude as is typically observed in geodynamo simulations (e.g. Christensen & Aubert 2006).

Our complete model thus comprises the angular momentum equations for the mantle (1), inner core (2) and the fluid cylinders (8), where  $\Gamma_g$  is specified by (4) and (5), and  $\Gamma_{\text{cmb}}$  and  $\Gamma_{\text{icb}}$  are specified by (11)–(21). We assume that  $\Omega_i$ ,  $\Omega_m$  and  $\Omega_f(s)$  are proportional to  $\exp(-i\omega t)$ . If no additional forcing is applied to this system, the solutions are free modes with (complex) frequencies  $\omega$  and (complex) eigenvectors specifying the relative amplitudes between  $\Omega_i$ ,  $\Omega_m$  and  $\Omega_f(s)$ . In the following sections we apply a forcing to these equations, also assumed to be proportional to  $\exp(-i\omega t)$ . This forcing is either applied directly on the mantle (added on the right-hand side of eq. 1), the inner core (right-hand side of eq. 2) or on cylinders inside the fluid core (right-hand side of eq. 8). With this added forcing, (complex) solutions of  $\Omega_i$ ,  $\Omega_m$  and  $\Omega_f(s)$  are found for given values of  $\omega$  and are proportional to the amplitude of the applied torque. Since the torque between any two regions depends on the product between a coupling strength and their differential rotation, large coupling strengths lead to small differential rotations. Thus regions that are strongly coupled together tend to be in corotation, though their angular velocities are never exactly identical as this would result in a vanishing torque.

### 3 THE DYNAMICS OF LOCKING

We consider the response of our coupling model to three different forcing scenarios. In the first, an equal and opposite torque is applied on the fluid cylinders that bracket the tangent cylinder. This scenario represents an approximation of the internal forcing that might occur due to convection in the fluid core and responsible for exciting free modes of torsional oscillations. The second scenario applies a torque solely to the inner core and is not meant to represent any physical situation but is useful for illustrating the range of system dynamics. The final scenario consists of a torque acting solely on the mantle, as might occur due to the tidal action of the oceans or some other external torque.

The model is solved for the complex angular velocities of the inner core, mantle and fluid core cylinders in response to the applied forcing at a given frequency. At sufficiently high frequency the choice of one thousand cylinders in the fluid core is insufficient to accurately resolve the system response; however, the model is well resolved for periods above 1 yr and we shall restrict our attention to those periods. We are interested in the effective locking of different regions within the core–mantle system, and in particular locking of the inner core to either the mantle or the fluid core within the tangent cylinder. For the fluid core we define the average velocities

of the region inside and outside the tangent cylinder as

$$\langle \Omega_c \rangle = \frac{1}{C_c} \int_0^{r_i} m(s) \Omega_f(s) ds, \quad (22)$$

$$\langle \Omega_o \rangle = \frac{1}{C_o} \int_{r_i}^{r_f} m(s) \Omega_f(s) ds, \quad (23)$$

where  $C_c$  and  $C_o$  are, respectively, the moments of inertia of the fluid inside and outside the tangent cylinder. If two regions within the system were perfectly locked, the ratio of their (complex) angular velocity amplitudes would be equal to one; if the regions oscillated with equal amplitude but exactly out of phase, this ratio would equal minus one.

We explore the behavior of our model for two different choices of inner core viscosity: a stiff inner core with a viscous relaxation time of  $\tau = 1000$  yr, and a softer inner core with  $\tau = 10$  yr. The results of these two models are presented in Figs 1 and 2, respectively.

All other model parameters are those of Table 1. We take the inner core as our reference body; in each figure, we plot the real part of the ratios of the mantle and fluid core velocities with respect to that of the inner core for a forcing applied at the tangent cylinder (top panel), solely on the inner core (middle panel) and solely on the mantle (bottom panel). All angular velocities in our model are linearly proportional to the amplitude of the imposed forcing; by considering angular velocity ratios as shown in Figs 1 and 2, our results are then independent of the forcing amplitude.

We begin our analysis with the case of the stiff inner core under the tangent cylinder forcing scenario (Fig. 1a). We are specifically interested in the efficiency with which the fluid part within the tangent cylinder can entrain the inner core, which is described by the ratio  $\Re(\langle \Omega_c \rangle / \Omega_i)$  (red line), and the degree to which the mantle is then entrained by the inner core, described by  $\Re(\Omega_m / \Omega_i)$  (green line). [The notation  $\Re(x)$  denotes the real part of  $x$ .] We find that the ratio  $\Re(\langle \Omega_c \rangle / \Omega_i)$  is close to 1 at all periods. At periods of a

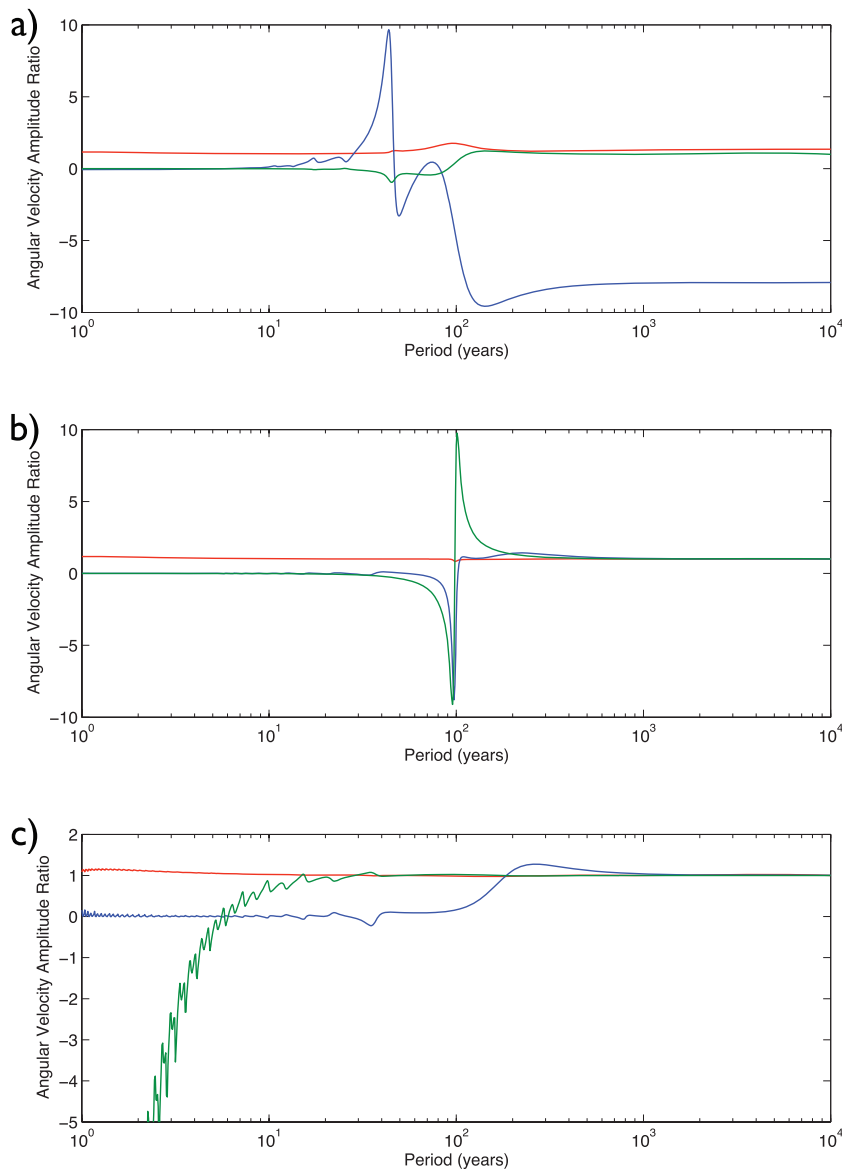


**Figure 1.** Angular velocities relative to that of the inner core for a forcing applied to the (a) tangent cylinder (b) inner core and (c) mantle. All panels show the velocities of the fluid inside the tangent cylinder (red lines), the fluid outside the tangent cylinder (blue lines) and the mantle (green lines). The viscous relaxation time of the inner core is  $\tau = 1000$  yr, all other parameters are as given in Table 1.

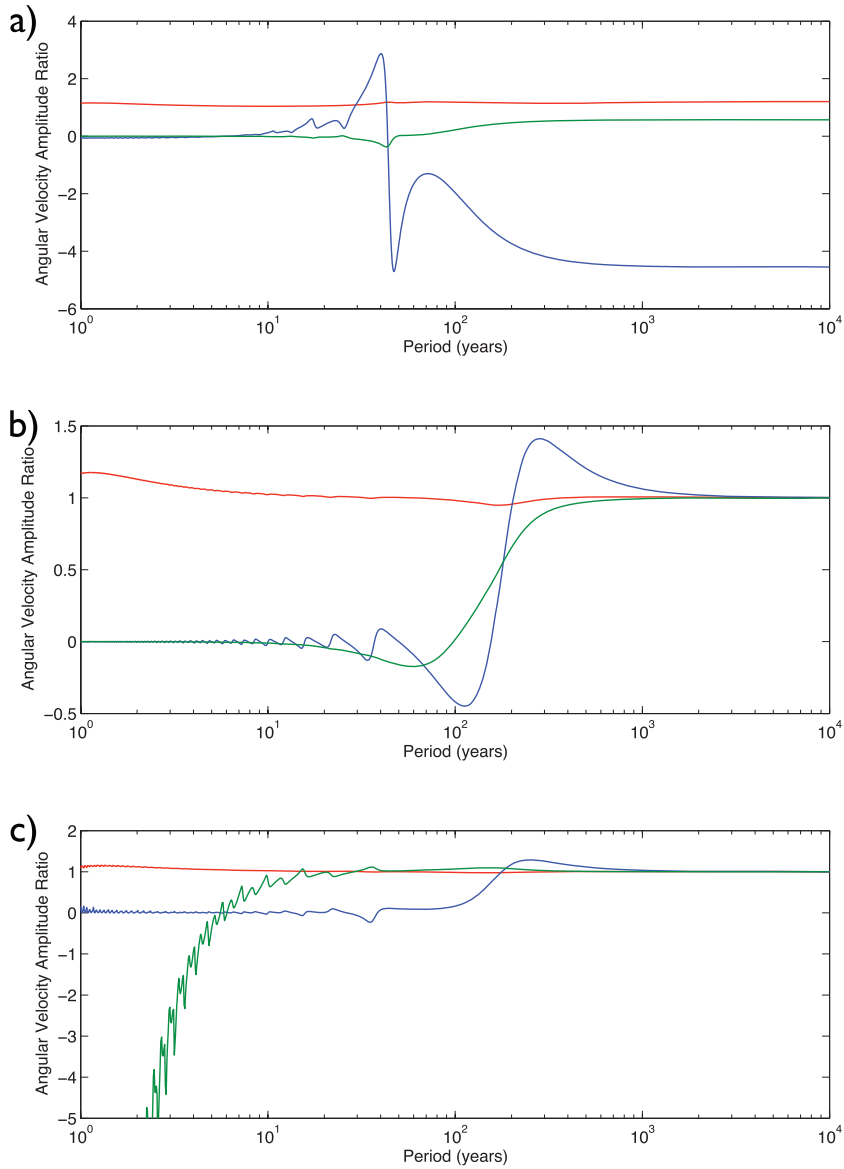


**Figure 2.** Angular velocities relative to that of the inner core for a forcing applied to the (a) tangent cylinder (b) inner core and (c) mantle. All panels show the velocities of the fluid inside the tangent cylinder (red lines), the fluid outside the tangent cylinder (blue lines) and the mantle (green lines). The viscous relaxation time of the inner core is  $\tau = 10$  yr, all other parameters are as given in Table 1.

few decades and smaller,  $\langle\Omega_c\rangle$  and  $\Omega_i$  differ by around 5 per cent. This is because EM coupling between the inner core and the fluid inside the tangent cylinder is sufficiently strong to effectively lock the two into corotation. The period at which locking occurs corresponds to the period of a free mode of oscillation between  $\Omega_i$  and  $\langle\Omega_c\rangle$  where the restoring torque between the two is EM (Gubbins 1981; Dumberry & Buffett 1999; Mound & Buffett 2003). The period of this free mode depends on the amplitude of the magnetic field at the ICB, occurring at shorter (longer) period for larger (smaller) field amplitude. For our values in Table 1, the period of this mode is approximately 0.3 yr. Beyond this period, the EM torque at the ICB overcomes the rotational inertia of the inner core and the latter is entrained by the fluid inside the tangent cylinder; the ratio  $\Re(\langle\Omega_c\rangle/\Omega_i)$  approaches 1 and the two are effectively locked together.

If the dynamics of the inner core and the fluid inside the tangent cylinder were only governed by EM coupling between the two,

$\Re(\langle\Omega_c\rangle/\Omega_i)$  would indeed be very close to one for all periods exceeding approximately 1 yr. This is clearly not the case, as evidenced by the deviation near periods of 100 yr where  $\Re(\langle\Omega_c\rangle/\Omega_i)$  increases to a peak value of 1.76. This deviation arises as a consequence of gravitational coupling between the inner core and the mantle, preventing the inner core to follow the fluid part of the tangent cylinder. Indeed, this is the location of the period of gravitational oscillation of the mantle with respect to a stationary inner core, the ‘abnormal’ mode identified in the previous section, whose period depends on the quantity  $\sqrt{\Gamma/C_m}$  and equals 97 yr for our choice of parameters. When the period of the forcing is larger than  $\sqrt{\Gamma/C_m}$ , the rotational inertia of the mantle can no longer resist the gravitational torque from the rotationally driven inner core. The inner core entrains the mantle into motion and the gravitational torque from the latter is no longer as effective to counteract the EM torque at the ICB; the ratio  $\Re(\langle\Omega_c\rangle/\Omega_i)$  decreases back towards 1. We find that  $\Re(\langle\Omega_c\rangle/\Omega_i) = 1.35$  for a periodic forcing of  $10^4$  yr.

The amplitude of the peak in  $\Re(\langle\Omega_c\rangle/\Omega_i)$  at the location of the ‘abnormal’ mode is determined by the relative strength between the gravitational and ICB couplings. A larger (smaller) magnetic field at the ICB would produce a less (more) prominent deviation from 1. Similarly, for a ‘softer’ inner core, and thus for a less effective gravitational coupling, the deviation from 1 is also reduced (compare the red lines of Figs 1 and 2).

The role of the mantle is confirmed by the way in which the ratio  $\Re(\Omega_m/\Omega_i)$  changes as a function of the period. At short periods,  $\Re(\Omega_m/\Omega_i)$  is very small, indicating that the mantle is not greatly involved in the angular momentum balance. As the period increases, the gravitational torque imparts larger accelerations on the mantle but it is not until the period reaches  $\sqrt{\bar{\Gamma}/C_m}$  that the inner core entrains the mantle into corotation. We have verified that the location of this transition period is indeed only a function of  $\sqrt{\bar{\Gamma}/C_m}$  and does not vary for different choices of magnetic field strength at the ICB and CMB, nor for different values of the  $B_s$ -field (and hence of the period of the free modes of torsional oscillations). Thus, the restoring torque for this ‘abnormal’ mode is entirely gravitational. (We note again that this is not a free mode of our system. The only gravitational free oscillation that our system supports is the MICG mode identified in Section 2.) At long periods, the mantle and inner core are closely, though not perfectly locked together ( $\Re(\Omega_m/\Omega_i) = 0.993$  at the longest periods considered).

Fluctuations in the amplitude of  $\Re(\langle\Omega_o\rangle/\Omega_i)$  (blue line) as the frequency of the forcing is varied occur due to the suite of torsional oscillation normal modes allowed by the system. For the chosen value of  $B_s$  the fundamental torsional oscillation mode has a period of 200 yr. Although it is difficult to see on the scale of the figure, the ratios  $\Re(\langle\Omega_c\rangle/\Omega_i)$  and  $\Re(\Omega_m/\Omega_i)$  also fluctuate as the period of the forcing comes into resonance with the torsional oscillation modes.

There is no net torque on the system for the tangent cylinder forcing scenario. The angular momentum of the whole Earth must be conserved which requires at least one region to rotate with opposite phase. Thus, while the whole tangent cylinder and mantle are moving approximately together in the long period limit, the fluid core outside the tangent cylinder is out of phase. The large amplitude of  $\langle\Omega_o\rangle$  is required in order to balance the larger moment of inertia of the combined mantle and tangent cylinder (compared to  $C_o$ ) and thus conserve angular momentum. For long periods we find that  $\Re(\langle\Omega_o\rangle/\Omega_i) = -7.91$ , which is slightly less than the ratio of moments of inertia  $(C_m + C_i + C_c)/C_o = 8.02$ . We would not expect these ratios to match exactly as the inner core, mantle and fluid within the tangent cylinder are not in perfect corotation.

We now consider the scenario in which a torque is applied solely to the inner core (Fig. 1b). For the entire range of periods considered the inner core and the fluid inside the tangent cylinder are approximately locked, although in this case it is the inner core that is entraining the fluid into motion. The locking of the mantle with the forced inner core oscillation occurs sharply at the 97-yr period. For the fluid outside the tangent cylinder, the EM coupling with the mantle exerts a larger influence than the coupling with the tangent cylinder. Thus, motions remain small until the 97-yr transition period when the mantle is set into motion by the inner core. At very long periods, due to the combination of the gravitational and EM coupling at the CMB, the motion of the entire planet oscillates approximately as a single rigid body in response to the forcing applied solely to the inner core; all ratios in the long period limit of Fig. 1(b) differ from 1 by at most one part in a thousand.

For a forcing applied solely to the mantle (Fig. 1c), the response of the core–mantle system is different. As is the case for a forcing

applied to the inner core, the inner core and fluid tangent cylinder are locked for the entire period range considered. At short periods, when the gravitational torque is not large enough to overcome the inertia of the whole of the tangent cylinder, the inner core motion remains small and as a result the amplitude of  $\Re(\Omega_m/\Omega_i)$  is large. The transition to locking between the mantle and the whole of the tangent cylinder occurs at much shorter periods compared to the inner core forcing scenario. This is because when the mantle is driving the motion, locking occurs when the gravitational coupling becomes larger than the rotational inertia of the whole of the tangent cylinder. This period is  $\sqrt{\bar{\Gamma}/(C_i + C_c)}$  and correspond approximately with that of the MICG mode.

The breadth of the resonance associated with the torsional oscillation normal modes prevents the period of the locking transition for this scenario from being as sharply defined as that for the inner core forcing scenario. The fluid outside the tangent cylinder is entrained into motion by EM coupling with the mantle, but it does not lock to the rest of the system until the period exceeds that of the fundamental mode of torsional oscillations of approximately 200 yr. At periods in excess of 1000 yr the system is effectively locked, with all ratios differing from 1 by at most one part in a thousand.

The periods of the locking transitions described above do not change when we consider a less viscous inner core (Fig. 2), although they are not as sharp as in the case with the stiffer inner core. For the forcing applied on the inner core and mantle we again have complete locking at the longest periods considered. For the tangent cylinder forcing scenario, although the locking transitions as a function of frequency do not change, the strength of the locking between the regions is now very different. In particular, in the long period limit, we find that  $\Re(\Omega_m/\Omega_i) = 0.57$ , and thus that there exists a significant differential rotation between the inner core and mantle. This is because as the inner core entrains the mantle by gravitational coupling, the motion of the latter is restricted by EM coupling at the CMB with the differentially rotating fluid core (we find  $\Re(\langle\Omega_o\rangle/\Omega_i) = -4.55$  at the longest period). By reducing the viscous relaxation timescale from 1000 to 10 yr, the strength of the gravitational coupling is now significantly decreased with respect to the EM coupling at the CMB, reducing the ability of the inner core to entrain the mantle in its motion.

The important message to take away from the above analysis is that for an external torque applied directly on the mantle or the inner core we expect the whole Earth to be corotating in the long period limit. However, in the case of an internally generated torque, conservation of angular momentum implies that at least one region must oscillate with a reversed phase. Which internal regions are corotating and which are in differential rotation is determined by the coupling strength between them. In particular, the inner core can rotate differentially with respect to the mantle if the strength of the coupling by surface forces on the CMB becomes comparable to that of the gravitational coupling.

#### 4 DIFFERENTIAL MOTION BETWEEN THE INNER CORE AND MANTLE

We now investigate in more detail the differential rotation between the inner core and mantle in order to determine the rotation rates that can be achieved by an oscillating inner core and to assess whether this can serve as an explanation for the seismically inferred inner core super-rotation. The absolute rates of rotation of every region are linearly proportional to the amplitude of the applied torque. Thus, a differential rotation of the inner core at the seismically inferred rate

can always be achieved by choosing appropriately the amplitude of the applied torque. However, we do not know a priori how large this torque can be. Moreover, the mantle oscillations generated in our model cannot be larger than the observed LOD variations. Therefore, we constrain the rates of inner core rotation, as was done in the study of Dumberry (2007), by renormalizing our results such that the resulting mantle oscillations equal  $0.005^\circ \text{ yr}^{-1}$ , corresponding to a 3 ms change in LOD. This represents approximately the largest observed LOD changes at decadal to millennial periods and sets a generous upper limit for the allowed inner core differential rotation. We use the same LOD constraint regardless of the frequency considered, though at periods close to 1 yr the observed LOD variations are at least an order of magnitude smaller.

The allowed inner core differential rotation, subject to the constraint that the observed LOD variations are not exceeded, can be expressed as

$$\Omega_i^{\text{diff}} = (0.005^\circ/\text{yr}) \times \left| \frac{\Omega_i}{\Omega_m} - 1 \right|. \quad (24)$$

This quantity is plotted in Fig. 3. As it was the case for Figs 1 and 2, the top, middle and bottom plots correspond to a torque applied at the tangent cylinder, on the inner core and on the mantle, respectively. We consider the same model parameters as in the previous section, as well as two additional models: one with no gravitational coupling and one in which the relaxation time of the inner core is only 1 yr. The horizontal dotted line in each panel of Fig. 3 corresponds to an inner core differential rotation of  $0.25^\circ \text{ yr}^{-1}$ . This is approximately the largest inner core rotation rate that is compatible with a number of different seismic observations (e.g. Tromp 2001; Song 2003), though it is possible that the true rate may be significantly smaller.

Not surprisingly, the mantle forcing scenario (Fig. 3c) is the least efficient in exciting rapid differential motion between the mantle and inner core. When constrained to not exceed 3 ms LOD variations, the mantle forcing scenario produces a differential rotation much smaller than  $0.25^\circ \text{ yr}^{-1}$  at all periods considered, regardless of the efficiency of gravitational coupling. Even amplification of the differential motion in the vicinity of the MICG mode or the torsional oscillation normal modes results in differential inner core rotation that is an order of magnitude below the seismically inferred rate.

In contrast, when the forcing is applied directly to the inner core (Fig. 3b), rotation rates of  $0.25^\circ \text{ yr}^{-1}$  or higher are possible. However, this is only the case for periods shorter than a few decades. Even in the absence of gravitational coupling, the inner core forcing scenario leads to differential rotation rates below  $0.25^\circ \text{ yr}^{-1}$  at periods longer than 100 yr. If gravitational coupling is present, the differential rotation is reduced significantly and rates of  $0.25^\circ \text{ yr}^{-1}$  are only possible at periods of a few decades or less. We recall that the relatively large rotation rates obtained at periods between 1 and 10 yr are misleading as subdecadal changes in LOD are at least an order of magnitude less than the 3 ms constraint that we have imposed.

The most dynamically relevant case for the Earth is the scenario with the forcing across the tangent cylinder (Fig. 3a), as this mimics internal torques that may occur within the fluid core and the Earth as a whole must conserve its own angular momentum. In the absence of gravitational coupling, a differential rotation in excess of  $0.25^\circ \text{ yr}^{-1}$  is achieved at all forcing periods. However, at periods longer than 10 yr, the inclusion of gravitational coupling greatly reduces the allowed differential rotation. The stiffer the inner core, the smaller is its differential rotation.

At periods between 10 and 100 yr, differential rotation rates as high as  $0.25^\circ \text{ yr}^{-1}$  cannot be achieved unless the viscous relaxation time of the inner core is approximately 1 yr or shorter, except at specific frequencies where a resonance with a torsional oscillation normal mode amplifies the differential rotation. Once more, the high rates at subdecadal periods are misleading.

When the forcing period is greater than all other timescales of our system (i.e. greater than the torsional oscillations modes,  $\tau$  and  $\sqrt{\bar{\Gamma}/C_m}$ ), the differential rotation of the inner core reaches an asymptotic rate which no longer depends on the forcing period. In this long period limit, for the parameters listed in Table 1, in order to achieve a differential rotation of  $0.25^\circ \text{ yr}^{-1}$ , the inner core relaxation time must be  $\sim 0.16$  yr. This corresponds to an inner core viscosity of  $\sim 1 \times 10^{16}$  Pa s, similar to the results obtained in the study of Dumberry (2007).

[We note that a different choice of internal forcing (i.e. a torque applied to different cylinders) does affect some of the details of the solutions presented in Fig. 3(a). However, we have verified that the general conclusions presented here are not greatly affected by the geometry of the internal forcing.]

The seismic observations suggest an eastward super-rotation of the inner core during the past 30 yr. Thus, if this is a reflection of an oscillating inner core, its period of oscillation would need to be at least twice as long (i.e. longer than 60 yr) and close to, or past the point where, the long period limit solution is applicable. It is possible to construct an analytical expression for  $\Omega_i^{\text{diff}}$  in this long period limit. This will also reveal how the differential rotation of the inner core depends explicitly on the parameters of our model. Combining eqs (1), (4) and (5) in the limit of  $d/dt \rightarrow 0$ , we obtain

$$\Gamma_{\text{cmb}} = -\bar{\Gamma} \tau (\Omega_i - \Omega_m). \quad (25)$$

Written in terms of averaged velocities  $\langle \Omega_o \rangle$  and  $\langle \Omega_c \rangle$ , the torque  $\Gamma_{\text{cmb}}$  defined in eqs (11) and (13) can be expressed as

$$\Gamma_{\text{cmb}} = \mathcal{F}_c (\langle \Omega_c \rangle - \Omega_m) + \mathcal{F}_o (\langle \Omega_o \rangle - \Omega_m), \quad (26)$$

where, using (15),  $\mathcal{F}_c$  and  $\mathcal{F}_o$  are defined by

$$\begin{aligned} \mathcal{F}_c &= \int_0^{r_i} \mathcal{F}_m \, ds \\ &= 2\pi G_m r_f^4 \left[ \frac{\langle B_m^m \rangle^2}{3} (2 - \zeta_1) + \frac{\langle B_m^d \rangle^2}{5} (2 - \zeta_2) \right] \end{aligned} \quad (27)$$

$$\begin{aligned} \mathcal{F}_o &= \int_{r_i}^{r_f} \mathcal{F}_m \, ds \\ &= 2\pi G_m r_f^4 \left[ \frac{\langle B_m^m \rangle^2}{3} \zeta_1 + \frac{\langle B_m^d \rangle^2}{5} \zeta_2 \right] \end{aligned} \quad (28)$$

with

$$\zeta_1 = (2 + r_{io}^2) (1 - r_{io}^2)^{1/2} \quad (29)$$

$$\zeta_2 = (2 + 3r_{io}^2) (1 - r_{io}^2)^{3/2} \quad (30)$$

$$r_{io} = \frac{r_i}{r_f}. \quad (31)$$

By assuming a locked tangent cylinder ( $\langle \Omega_c \rangle = \Omega_i$ ) and conservation of angular momentum from which

$$\langle \Omega_o \rangle = - \left( \frac{C_i + C_c}{C_o} \right) \Omega_i - \frac{C_m}{C_o} \Omega_m, \quad (32)$$

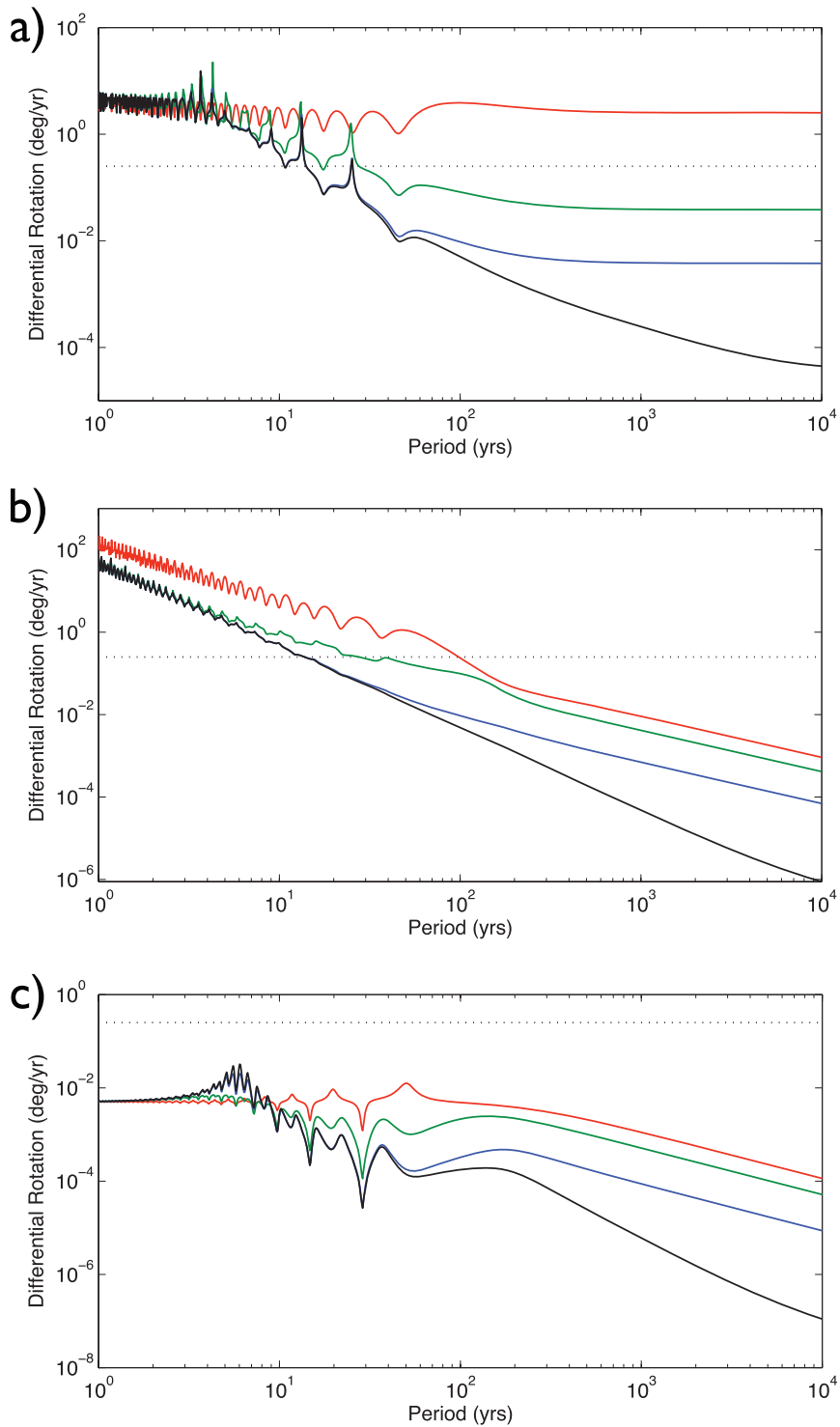


**Figure 3.** Amplitudes of inner core differential rotation for oscillatory motion subject to the constraint that LOD changes do not exceed 3 ms in amplitude at the given period. We consider models with no gravitational coupling (red lines), and gravitational coupling with an inner core relaxation time of 1 yr (green lines), 10 yr (blue lines) or 1000 yr (black lines). The dotted horizontal lines indicate an inner core differential rotation of  $0.25^\circ \text{ yr}^{-1}$ . As in previous figures, we consider a forcing applied to the (a) tangent cylinder (b) inner core and (c) mantle.

the combination of (25) and (26) yields

$$\frac{\Omega_i}{\Omega_m} = \frac{\bar{\Gamma}\tau + \mathcal{F}_c + \mathcal{F}_o \left( \frac{C_m}{C_o} + 1 \right)}{\bar{\Gamma}\tau + \mathcal{F}_c - \mathcal{F}_o \left( \frac{C_i + C_c}{C_o} + 1 \right)}. \quad (33)$$

We find that substituting this approximation into (24) provides a very good match, in the long period limit, to the solutions of our model such as those presented in Fig. 3(a).

The analytical expression (33) allows us to determine the required combination of parameters such that a rate of  $0.25^\circ \text{ yr}^{-1}$  can be

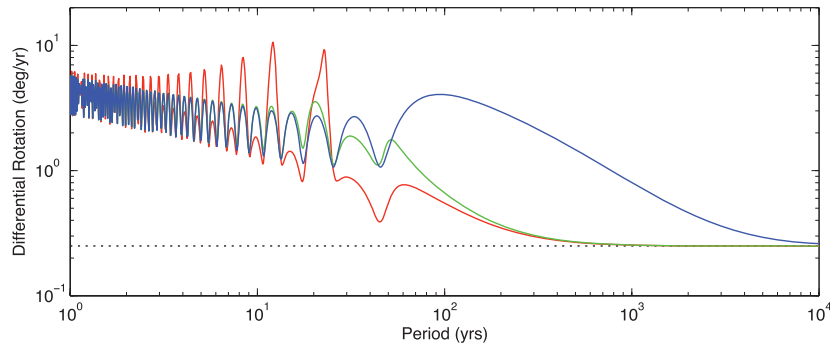


**Figure 4.** Amplitudes of inner core differential rotation for a forcing applied to the tangent cylinder subject to the constraint that LOD changes do not exceed 3 ms in amplitude at the given period. Three different sets of gravitational coupling parameters are shown:  $\bar{\Gamma} = 3 \times 10^{20}$  N m and  $\tau = 0.166$  yr (red line);  $\bar{\Gamma} = 5 \times 10^{18}$  N m and  $\tau = 10$  yr (green line);  $\bar{\Gamma} = 1 \times 10^{17}$  N m and  $\tau = 500$  yr (blue line). Other parameters are as given in Table 1. The dotted horizontal lines indicate an inner core super-rotation of  $0.25^\circ \text{ yr}^{-1}$ .

achieved in the long period limit. If we use the ‘typical’ EM coupling parameters given in Table 1, then  $\mathcal{F}_c = 8.81 \times 10^{25}$  N m s and  $\mathcal{F}_o = 8.05 \times 10^{27}$  N m s. In order to get  $\Omega_i^{\text{diff}} = 0.25^\circ \text{ yr}^{-1}$ , the product of  $\bar{\Gamma}$  and  $\tau$  must then be equal to approximately  $1.6 \times 10^{27}$  N m s or, equivalently, to  $5 \times 10^{19}$  N m yr. Different combinations of  $\bar{\Gamma}$  and  $\tau$  affect the dynamics of gravitational coupling, notably the periods of the MICG and ‘abnormal’ modes, but  $\Omega_i^{\text{diff}}$  should not change in the long period limit. This is illustrated in Fig. 4 where we show  $\Omega_i^{\text{diff}}$  computed for the tangent cylinder forcing scenario for three different combinations of  $\bar{\Gamma}$  and  $\tau$ , but each with a product equal to  $5 \times 10^{19}$  N m yr. The three cases shown are for:  $\bar{\Gamma} = 3 \times 10^{20}$  N m and  $\tau = 0.166$  yr (red line);  $\bar{\Gamma} = 5 \times 10^{18}$  N m and  $\tau = 10$  yr (green line);  $\bar{\Gamma} = 1 \times 10^{17}$  N m and  $\tau = 500$  yr (blue line). The periods of the MICG and the ‘abnormal’ modes for each of these three cases are, respectively: 6.1 and 97 yr; 48 and 751 yr; 336 and 5312 yr. No marked transitions at these periods can be seen on Fig. 4 because the inner core viscous relaxation time is smaller than both of these periods for the red and green curves and approximately equal to the MICG period for the blue curve. In all cases, the differential rotation of the inner core in the long period limit is  $0.25^\circ \text{ yr}^{-1}$ , in agreement with our analytical expression based on (33).

Fig. 4 thus illustrates that it is possible to achieve  $\Omega_i^{\text{diff}} = 0.25^\circ \text{ yr}^{-1}$  with an oscillating inner core without violating the observed LOD variations. For this to be the case, using the typical EM coupling parameters, the condition on the gravitational coupling parameters is that the combination  $\bar{\Gamma}\tau$  must be less or equal to  $5 \times 10^{19}$  N m yr. A larger EM coupling strength at the CMB allows larger values of  $\bar{\Gamma}\tau$  to be compatible with  $\Omega_i^{\text{diff}} = 0.25^\circ \text{ yr}^{-1}$ . As explained in Section 3, this is because as the inner core entrains the mantle by gravitational coupling, the motion of the latter is restricted by EM coupling with the fluid core at the CMB. Thus, the larger the EM coupling, the lesser the entrainment of the mantle by the inner core, resulting in a greater differential rotation between the two. A larger EM coupling can be accomplished either by an increase in the conductance or an increase in the amplitude of the magnetic field at the CMB. We do not present solutions here for different scenarios of EM coupling, though using (33), we can determine that, for instance if  $\bar{\Gamma} = 3 \times 10^{20}$  N m,  $\tau = 5$  yr, and  $\langle B_m^m \rangle$  and  $\langle B_m^d \rangle$  are as given in Table 1, in order to have  $\Omega_i^{\text{diff}} = 0.25^\circ \text{ yr}^{-1}$ , the conductance at the base of the mantle would need to be increased to  $3 \times 10^9$  S. This is similar to the conclusion reached in the study of Dumberry (2007).

## 5 DISCUSSION AND CONCLUSION

Our investigation has shown how the entrainment of the inner core, mantle and fluid core into motion for a given forcing scenario depends on the strength of the coupling between these regions relative to their rotational inertia. EM coupling at the ICB ensures that the inner core and the fluid inside the tangent cylinder are generally locked for periods larger than approximately 1 yr. Gravitational coupling between the mantle and inner core also ensures eventual locking between the two if the forcing is applied directly on either of them. However, because of their very different moment of inertia, the period at which this locking occurs depends on which of the two is driving the motion.

For an external forcing applied to the mantle, the inner core (together with the fluid inside the tangent cylinder) is expected to be locked to the motion of the mantle at periods longer than  $\sqrt{\bar{\Gamma}/(C_i + C_c)}$ , approximately equal to the period of the MICG mode. The exact value of this period depends on  $\bar{\Gamma}$ ; for  $\bar{\Gamma} = 3 \times 10^{20}$  N m (Mound & Buffett 2006) it is equal to 6.1 yr. Possible physical sources of mantle forcing include angular momentum exchange with the oceans and atmosphere (e.g. Dickey *et al.* 2003), or tidal breaking (e.g. Christodoloudis *et al.* 1988). We thus expect that if the timescale of the mantle forcing exceeds a few decades, the small rotational inertia of the inner core implies that it cannot resist the gravitational torque from the mantle and is forced to rotate in unison with it. On this basis, the seismically observed inner core super-rotation cannot represent a fossil rotation rate, either from tidal despinning that has not yet been transmitted to the inner core or from mantle spin changes associated with quaternary glaciations (e.g. Bills 1999).

If, however, the changes in rotation are imposed by torques on the inner core, it is only for periods longer than  $\sqrt{\bar{\Gamma}/C_m}$  that the mantle becomes gravitationally locked to the inner core. For  $\bar{\Gamma} = 3 \times 10^{20}$  N m, this period is 97 yr. At smaller periods, the rotational inertia of the mantle is larger than the gravitational torque from the inner core and this prevents gravitational locking.

The forcing scenario that is the most relevant for the Earth is one where changes in rotation result from internal torques within the fluid core. If the strength of gravitational coupling is large, for periods longer than  $\sqrt{\bar{\Gamma}/C_m}$  the inner core efficiently entrains the mantle and the differential rotation between the two is limited. However, in this scenario, the bulk of the fluid core outside the tangent cylinder must rotate in the reverse direction in order to conserve

the angular momentum of the whole Earth. Coupling between the fluid core and the mantle from surface forces at the CMB can thus prevent the mantle from being fully gravitationally entrained by the inner core. A relatively high coupling at the CMB compared to the gravitational coupling may thus allow a significant differential rotation between the inner core and the mantle.

Assuming EM coupling at the CMB of typical strength (based on a lower mantle conductance of  $10^8$  S and a magnetic field amplitude consistent with a downward continuation of the field observed at the Earth's surface), in order to explain a differential rotation as high as  $0.25^\circ \text{ yr}^{-1}$  (e.g. Zhang *et al.* 2005) in terms of an oscillating inner core, the condition on the gravitational coupling is  $\bar{\Gamma}\tau \leq 5 \times 10^{19}$  N m yr. Larger values of  $\bar{\Gamma}\tau$  would require a proportionally larger coupling strength at the CMB. If these constraints are not met, an oscillating inner core at a rate of  $0.25^\circ \text{ yr}^{-1}$  would lead to larger LOD changes than those observed. These constraints are broadly similar to those derived in the study of Dumberry (2007), where a simplified model of the fluid core was used. Thus, the inclusion of torsional oscillations in the fluid core, as done in the present study, do not alter significantly the dynamics of internal coupling at long periods.

The condition  $\bar{\Gamma}\tau \leq 5 \times 10^{19}$  N m yr represents a weaker gravitational coupling than previous estimates. The parameter  $\bar{\Gamma}$  depends on the amplitude of the geoid undulations produced by density anomalies in the mantle (including topography at the CMB) and the density structure of the inner core (which should align with the imposed mantle geoid on long timescales). It has been proposed that a periodic 6-yr signal in the LOD variations (Abarca del Rio *et al.* 2000) represents the MICG mode, in which case  $\bar{\Gamma}$  cannot depart much from  $3 \times 10^{20}$  N m (Mound & Buffett 2006). As a reference, this corresponds to degree 2 geoid undulations of approximately 300 m along the equator of the CMB, compatible with some geodynamic models (Forte & Peltier 1991; Defraigne *et al.* 1996). For a 6-yr MICG mode to be observed,  $\tau$  must be at least  $\sim 5$  yr or larger, otherwise it would be rapidly attenuated. This leads to  $\bar{\Gamma}\tau \geq 1.5 \times 10^{21}$  N m yr, much larger than the condition we have derived above.

Using the lowest possible value of  $\bar{\Gamma}\tau$  consistent with the interpretation of the 6-yr LOD signal in terms of the MICG mode,  $\bar{\Gamma}\tau = 1.5 \times 10^{21}$  N m yr, together with our typical EM coupling strength, the possible inner core oscillation rates at periods longer than 100 yr cannot exceed  $0.01^\circ \text{ yr}^{-1}$ . If these parameters are correct, the implication is that the seismically inferred rates of inner core differential rotation cannot represent a long period oscillation. Larger rates of differential inner core rotation are possible for larger EM coupling at the CMB. Rates as high as  $0.25^\circ \text{ yr}^{-1}$  can be produced if we increase the mantle conductance to  $3 \times 10^9$  S. While not completely implausible, such a high conductance would act as an effective filter on the secular variation of the core field observed at the surface. It is thus difficult to reconcile a conductance this large with observed monthly changes in the core field detected in satellite observations (Olsen & Manda 2008). Alternately, since EM coupling varies with the square of the rms radial magnetic field at the CMB (see eq. 15), a value of the latter larger than 0.32 mT based on downward continuation of the surface field would also increase the amplitude of EM coupling. Indeed, significant energy may be present in the small-scale components of the CMB field, a part of the spectrum that is not accessible from surface observation because it is masked by the crustal field. Studies of forced nutations suggest that the rms value of the magnetic field at the CMB may be closer to 0.7 mT (Mathews *et al.* 2002). Adopting such a radial field strength, and  $\bar{\Gamma}\tau = 1.5 \times 10^{21}$  N m yr, the mantle conductance

required to get  $\Omega_i^{\text{diff}} = 0.25^\circ \text{ yr}^{-1}$  is reduced to  $7.5 \times 10^8$  S, less in conflict with magnetic field observations.

Such a high EM coupling scenario would thus allow us to explain the seismic rates of inner core rotation in terms of a long period ( $> 100$  yr) oscillation while not being in conflict with a gravitational coupling strength based on a 6-yr MICG mode. However, this would still require an inner core viscous relaxation time not much larger than 5 yr, corresponding to an inner core viscosity of  $\sim 2.5 \times 10^{17}$  Pa s. For a weaker CMB coupling than this high EM coupling scenario, an oscillating inner core at a differential rate of  $0.25^\circ \text{ yr}^{-1}$  implies that  $\bar{\Gamma}\tau < 1.5 \times 10^{21}$  N m yr, and thus either  $\bar{\Gamma} < 3 \times 10^{20}$  N m, or  $\tau < 5$  yr, or both, in which case the 6-yr LOD signal cannot represent the MICG mode and therefore must be from a different origin. This would also indicate that the amplitude of the long-wavelength geoid at the CMB is smaller than 300 m, perhaps in better agreement with more recent geodynamic models (Simmons *et al.* 2006).

In summary, an explanation of the differential inner core rotation in terms of a long period oscillations is possible, but it requires either a low gravitational coupling strength, a higher EM coupling strength than our typical estimate, or both.

If the present-day eastward inner core super-rotation is part of a slow oscillation, or slow fluctuations, the timescale of these remains uncertain. As noted in the introduction, a steady rotation poses a problem if the hemispherical anisotropy structure of the inner core results from a process controlled by the mantle. One must then make sure that fluctuations would also not take the inner core too far out of alignment with the mantle. An inner core oscillating at a peak rate of  $0.2^\circ \text{ yr}^{-1}$  and a period of 100 yr would lead to a peak-to-peak longitudinal angular displacement of  $\sim 6^\circ$ . If the period is 1000 yr, the peak-to-peak angular displacement is  $\sim 60^\circ$ . Such longitudinal fluctuations are not insignificant, but may remain compatible with an inner core anisotropy mechanism requiring a general alignment with the mantle.

Though our model allows us to calculate the rotation rates at any period, it is important to note that our calculation at millennial timescales and beyond must be regarded with suspicion for two reasons. First, the results presented here use a model of torsional oscillations in which magnetic diffusion within the fluid core is not taken into account; magnetic diffusion should play a role at millennial timescales. A more fundamental issue though is that purely rigid flows may no longer be an appropriate description of the fluid core dynamics; variations in thermal winds, a type of flow involving axial gradients, may be significant at millennial timescales.

Coupling of the inner core to millennial timescale variations in thermal wind could then serve as an alternate mechanism to explain the seismically observed inner core super-rotation. Indeed, the presence of such variations has been suggested on the basis of the observed archaeomagnetic secular variation and millennial LOD changes (Dumberry & Bloxham 2006; Dumberry & Finlay 2007). A thermal wind flow may have opposite flow directions at the ICB and CMB, and thus have the ability to apply torques in opposite directions on the mantle and inner core: this would naturally promote a higher differential rotation between the two.

## ACKNOWLEDGMENTS

Mathieu Dumberry is currently supported by a NSERC/CRSNG discovery grant. Jon Mound recognizes support of the WUN-Leeds Fund for International Research Collaboration.

## REFERENCES

- Abarca del Rio, R., Gambis, D. & Salstein, D.A., 2000. Interannual signals in length of day and atmospheric angular momentum, *Ann. Geophys.*, **18**, 347–364.
- Aubert, J., Amit, H., Hulot, G. & Olson, P., 2008. Thermochemical flows couple the Earth's inner core growth to mantle heterogeneity, *Nature*, **454**(7205), 758–761.
- Bills, B., 1999. Tidal despinning of the mantle, inner core superrotation, and outer core effective viscosity, *J. geophys. Res.*, **104**, 2653–2666.
- Braginsky, S.I., 1970. Torsional magnetohydrodynamic vibrations in the Earth's core and variations in day length, *Geomag. Aeron.*, **10**, 1–10.
- Buffett, B.A., 1996. Gravitational oscillations in the length of the day, *Geophys. Res. Lett.*, **23**, 2279–2282.
- Buffett, B.A., 1997. Geodynamic estimates of the viscosity of the Earth's inner core, *Nature*, **388**, 571–573.
- Buffett, B.A., 1998. Free oscillations in the length of day: inferences on physical properties near the core–mantle boundary, in *The Core–Mantle Boundary Region*, Vol. 28 of Geodynamics series, pp. 153–165, eds Gurnis, M., Wyssession, M.E., Knittle, E. & Buffett, B.A., AGU Geophysical Monograph, Washington, DC.
- Buffett, B.A., Mound, J. & Jackson, A., 2009. Inversion of torsional oscillations for the structure and dynamics of earth's core, *Geophys. J. Int.*, **177**, 878–890.
- Christensen, U.R. & Aubert, J., 2006. Scaling properties of convection-driven dynamos in rotating spherical shells and application to planetary magnetic fields, *Geophys. J. Int.*, **166**, 97–114.
- Christodoulidis, D.C., Smith, D.E., Williamson, R.G. & Klosko, S.M., 1988. Observed tidal breaking in the Earth/Moon/Sun system, *J. geophys. Res.*, **93**, 6216–6236.
- Defraigne, P., Dehant, V. & Wahr, J.M., 1996. Internal loading of an inhomogeneous compressible Earth with phase boundaries, *Geophys. J. Int.*, **125**, 173–192.
- Dickey, J.O., Marcus, S.L. & de Viron, O., 2003. Coherent interannual and decadal variations in the atmosphere–ocean system, *Geophys. Res. Lett.*, **30**, 1573, doi:10.1029/2002GL016763.
- Dumberry, M., 2007. Geodynamic constraints on the steady and time-dependent inner core axial rotation, *Geophys. J. Int.*, **170**, 886–895.
- Dumberry, M. & Bloxham, J., 2006. Azimuthal flows in the Earth's core and changes in length of day at millennial timescales, *Geophys. J. Int.*, **165**, 32–46.
- Dumberry, M. & Buffett, B.A., 1999. On the validity of the geostrophic approximation for calculating the changes in the angular momentum of the core, *Phys. Earth planet. Inter.*, **112**, 81–89.
- Dumberry, M. & Finlay, C.C., 2007. Eastward and westward drift of the earth's magnetic field for the last three millennia, *Earth planet. Sci. Lett.*, **254**, 146–157.
- Dumberry, M. & Mound, J.E., 2008. Constraints on core–mantle electromagnetic coupling from torsional oscillation normal modes, *J. geophys. Res.*, **113**, B03102, doi:10.1029/2007JB005135.
- Forte, A.M. & Peltier, R., 1991. Viscous flow models of global geophysical observables 1. forward problems, *J. geophys. Res.*, **96**(B12), 20 131–20 159.
- Glatzmaier, G.A. & Roberts, P.H., 1996. Rotation and magnetism of Earth's inner core, *Science*, **274**, 1887–1891.
- Gubbins, D., 1981. Rotation of the inner core, *J. geophys. Res.*, **86**, 11 695–11 699.
- Gubbins, D. & Roberts, P.H., 1987. Magnetohydrodynamics of the Earth's core, in *Geomagnetism*, Vol. 2, pp. 1–184, ed. Jacobs, J.A., Academic Press, London.
- Jackson, A., Bloxham, J. & Gubbins, D., 1993. Time-dependent flow at the core surface and conservation of angular momentum in the coupled core–mantle system, in *Dynamics of the Earth's Deep Interior and Earth Rotation*, Vol. 72, pp. 97–107, eds Le Mouél, J.-L., Smylie, D.E. & Herring, T., AGU Geophysical Monograph, Washington, DC.
- Jackson, A., Jonkers, A.R.T. & Walker, M.R., 2000. Four centuries of geomagnetic secular variation from historical records, *Phil. Trans. R. Soc. Lond., A*, **358**, 957–990.
- Jault, D., Gire, C. & Le Mouél, J.-L., 1988. Westward drift, core motions and exchanges of angular momentum between core and mantle, *Nature*, **333**, 353–356.
- Mathews, P.M., Herring, T.A. & Buffett, B.A., 2002. Modeling of nutations and precession: new nutation series for nonrigid Earth and insights into the Earth's interior, *J. geophys. Res.*, **107**, doi:10.1029/2004JB000390.
- Mound, J.E. & Buffett, B.A., 2003. Interannual oscillations in the length of day: implications for the structure of mantle and core, *J. geophys. Res.*, **108**(B7), 2334, doi:10.1029/2002JB002054.
- Mound, J.E. & Buffett, B.A., 2005. Mechanisms of core–mantle angular momentum exchange and the observed spectral properties of torsional oscillations, *J. geophys. Res.*, **110**, B08103, doi:10.1029/2004JB003555.
- Mound, J.E. & Buffett, B.A., 2006. Detection of a gravitational oscillation in length-of-day, *Earth planet. Sci. Lett.*, **243**, 383–389.
- Niu, F. & Wen, L., 2001. Hemispherical variations in seismic velocity at the top of the Earth's inner core, *Nature*, **410**(6832), 1081–1084.
- Olsen, N. & Manda, M., 2008. Rapidly changing flows in the Earth's core, *Nature Geosc.*, **1**, 390–394.
- Simmons, N.A., Forte, A.M. & Grand, S.P., 2006. Constraining mantle flow with seismic and geodynamic data: a joint approach, *Earth planet. Sci. Lett.*, **246**, 109–124.
- Song, X., 2003. Three-dimensional structure and differential rotation of the inner core, in *Earth's Core: Dynamics, Structure, Rotation*, Vol. 31 of Geodynamics series, pp. 45–64, eds Dehant, V., Creager, K.C., Karato, S.-I. & Zatman, S., AGU Geophysical Monograph.
- Sreenivasan, B. & Gubbins, D., 2008. Dynamos with weakly convecting outer layers: implications for core–mantle boundary interaction, *Geophys. Astrophys. Fluid Dyn.*, **102**(4), 395–407.
- Stacey, F.D., 1992. *Physics of the Earth*, 3rd edn, Brookfield Press, Kenmore, Australia.
- Stacey, F.D. & Anderson, O.L., 2001. Electrical and thermal conductivities of Fe–Ni–Si alloy under core conditions, *Phys. Earth planet. Inter.*, **124**, 153–162.
- Sumita, I. & Bergman, M.I., 2007. Inner core dynamics, in *Treatise on Geophysics*, Vol. 8, chap. 10, pp. 299–318, eds Schubert, G. & Olson, P., Elsevier, Amsterdam.
- Tanaka, S. & Hamaguchi, H., 1997. Degree one heterogeneity and hemispherical variation in anisotropy in the inner core from PKP(BC)–PKP(DF) times, *J. geophys. Res.*, **102**, 2925–2938.
- Taylor, J.B., 1963. The magneto-hydrodynamics of a rotating fluid and the Earth's dynamo problem, *Proc. R. Soc. Lond., A*, **274**, 274–283.
- Tromp, J., 2001. Inner-core anisotropy and rotation, *Ann. Rev. Earth planet. Sci.*, **29**, 47–69.
- Willis, A., Sreenivasan, B. & Gubbins, D., 2007. Thermal core–mantle interaction: exploring regimes for 'locked' dynamo action, *Phys. Earth planet. Inter.*, **165**(1–2), 83–92.
- Zatman, S. & Bloxham, J., 1997. Torsional oscillations and the magnetic field within the Earth's core, *Nature*, **388**, 760–763.
- Zhang, J., Song, X., Li, Y., Richards, P.G., Sun, X. & Waldhauser, F., 2005. Inner core differential motion confirmed by earthquake waveform doublets, *Science*, **309**, 1357–1360.